Controllable Synthesis of Atomic Sn-anchored Carbon Host for Excellent Long-Cycle-Life Zinc Metal Batteries

*Lantao Liu [a, b, c, 1], Yiming Li [a, 1], Hu Zhang [b], Fang Dong [c], Shuaize Wang [a], Ziyu Sun [a], Gaixia Zhang [d, *], Xiaohong Chen [a, *], Sasha Omanovic [b], Shuhui Sun [c, *], and Huaihe Song [a, *]*

a State Key Laboratory of Chemical Resource Engineering, Beijing Key Laboratory of Electrochemical Process and Technology for Materials, Beijing University of Chemical Technology, Beijing, 100029, P. R. China.

b Department of Chemical Engineering, McGill University, 3610 Rue University, Quebec H3A 0C5, Canada.

c Institut National de la Recherche Scientifique (INRS), Énergie Matériaux Télécommunications Research Centre, Québec J3X 1P7, Canada.

d Department of Electrical Engineering, École de Technologie Supérieure (ÉTS), Montréal, Québec H3C 1K3, Canada.

E-mail: gaixia.zhang@etsmtl.ca, chenxh@mail.buct.edu.cn, shuhui.sun@inrs.ca, songhh@mail.buct.edu.cn.

Author Contributions

The manuscript was written through contributions of all authors. All authors have given approval to the final version of the manuscript.

Notes

The authors declare no competing financial interest.

Acknowledgements

This work was supported by the National Natural Science Foundation of China (51972014).

Experimental Section

Synthesis of HMCS: 50 mg F-127 (average Mn-13000, Macklin) was dissolved in 60 ml deionized water and then stirred for 20 min. Subsequently, 0.38 mL aniline (AR, 99.5 %, Aladdin) and 0.29 ml pyrrole (99 %, Aladdin) were added to the mixed solution and stirred for 30 min (A). Then, 1.917 g ammonium persulfate (APS) (99.99%, Aladdin) was dissolved in 5 ml deionized water and then stirred for 15 min (B). Next, let A and B stand still for 1 h at 5 ℃ in incubator to initiate the polymerization of the precursor. Then mixed them quickly with magnetic stirring for 40 s. The mixed solution was put in incubator under 5 ℃ for 24 h. The product was repeated washed with ethanol and water by suction filtration, and then put it in vacuum oven at 80 ℃ for 24 h. Finally, put the product to a tube furnace and heated to 700 ℃ with a heating rate of 5 ℃ min^{-1} under N_2 atmosphere and kept for 2 h to obtain the HMCS.

Synthesis of Sn@HMCS: 70 mg F-127 (average Mn-13000, Macklin) was dissolved in 60 ml deionized water and then stirred for 20 min. Subsequently, 0.49 mL aniline (AR, 99.5 %, Aladdin) and 0.38 ml pyrrole (99 %, Aladdin) were added to the mixed solution and stirred for 30 min (A). Then, 2.47 g ammonium persulfate (APS) (99.99%, Aladdin) was dissolved in 5 ml deionized water and then stirred for 15 min (B). Then, 0.9 g $SnCl_2$ and 0.3g thiourea (99.99%, Aladdin) was dissolved in 30 ml deionized water and then stirred for 30 min (C). Next, take 4ml of C and add it to A and stir for 20 min (D). Finally, let D and B stand still for 50 min at 0 °C in incubator to initiate the polymerization of the precursor. Then mixed them quickly with magnetic stirring for 1 min. The mixed solution was put in incubator under 0 °C for 24 h. The product was repeated washed with ethanol and water by suction filtration, and then put it in vacuum oven at 80 °C for 24 h. Finally, put the product in a tube furnace and heated to 700 °C with a heating rate of 5 °C min^{-1} under N_2 atmosphere and kept for 3 h to obtain the Sn@HMCS.

Preparation of MnO_2: Prepare 0.1 M aqueous solution of $KMnO_4$ and 0.6 M aqueous solution of $MnSO_4 \cdot H_2O$, take 15 mL of each, add the latter to the aqueous solution of the former, and stir for 30 min. Transfer the solution to a hydrothermal kettle and hold it for 12 hours (160 °C). The supernatant was removed first, and then the brown solid at the bottom was divided into two homogeneous parts and transferred into two 50 mL centrifugal tubes for centrifugation for 5 min. The brown homogenate was cleaned several times and dried in a vacuum oven (80 degrees, 12 hours) to finally get pure MnO_2.

Characterization: The morphology and microstructure were studied by scanning electron microscopy (ZEISS SUPRATM) and transmission electron microscopy (Hitachi 7700). The composition information was tested by Thermogravimetric (NETZSCH), and X-ray photoelectron spectra (ESCALAB250 electron spectrometer). The crystal structure was studied by X-ray diffraction (Rigaku D), and Raman spectroscopy (Aramis, Jobin Yvon). The surface structure was tested using N_2 adsorption-desorption (Micromeritics ASAP 2020).

Calculation details: The calculation details refer to our previous work for details.[1]

Electrochemical measurements: The Sn@HMCS and sodium alginate (SA) (AR, 90 %, Macklin) were mixed in deionized water with mass ratio of 90:10, and then coated on Cu foil. After drying at 120 °C for 12 h, Sn@HMCS electrode was obtained. The HMCS electrode was prepared in the same way. The MnO_2 electrode was prepared by mixing MnO_2, Acetylene black, and polyvinylidene difluoride (PVDF) with mass ratio of 7:2:1 in N-Methyl pyrrolidone (NMP) and coated on Stainless steel mesh.

All the zinc metal cells are constructed in a coin-type cell (CR2032). The half cells are constructed with Zn plate as anode and Sn@HMCS as cathode. 2 M $ZnSO_4$ and 0.5 M $NaSO_4$ are used as electrolyte. The active material mass of the electrode sheet used in the half battery is 0.8-1.2 mg. The pre-Zn deposition Sn@HMCS acts as the anode and cathode of symmetrical cells. The electrolyte of symmetrical cells is the same as that of half cells. The specific deposition process is as follows: Zinc is deposited on the anode of Sn@HMCS with a deposition surface capacity of 8 mAh cm^{-2} by the method of constant current deposition (1 mA cm^{-2}). The electrolyte of the Zn-MnO_2 full cell is 2 M $ZnSO_4$ and 0.1 M $MnSO_4$, the anode is same as the symmetrical cell anode. The load of MnO_2 in the full cell is 1.5-3 mg. The capacity of pre-deposited zinc is 6.28 mAh. The anode/cathode capacity ratio is 6.79.

The galvanostatic charge-discharge (GCD) and cyclic voltammetry (CV) were studied on CHI 760 E electrochemical workstation (Shanghai Chenhua) and CT2001A test instrument (Wuhan LAND), respectively. The electrochemical impedance spectroscopy (EIS) tests were tested on electrochemical workstation in the frequency range of 0.01 – 100000 Hz with an amplitude of 1.2 V. For the half cells tests, the voltage window was 0.01 – 0.2 V. And the voltage window of full cells was 0.8 – 1.8 V.

The energy density (E, Wh kg^{-1}) and power density (P, W kg^{-1}) of full cells were calculated by the following equations based on the active material mass of cathodes:

$$E = C * V$$

$$P = \frac{E}{t}$$

where C, V, t represents the specific discharge capacity, average discharge voltage, time for discharge, respectively.

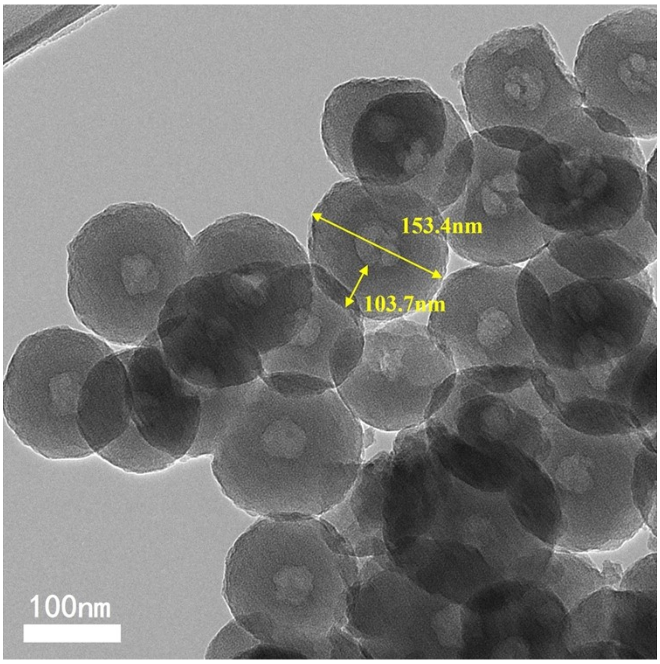

Figure S1. TEM image of HMCS.

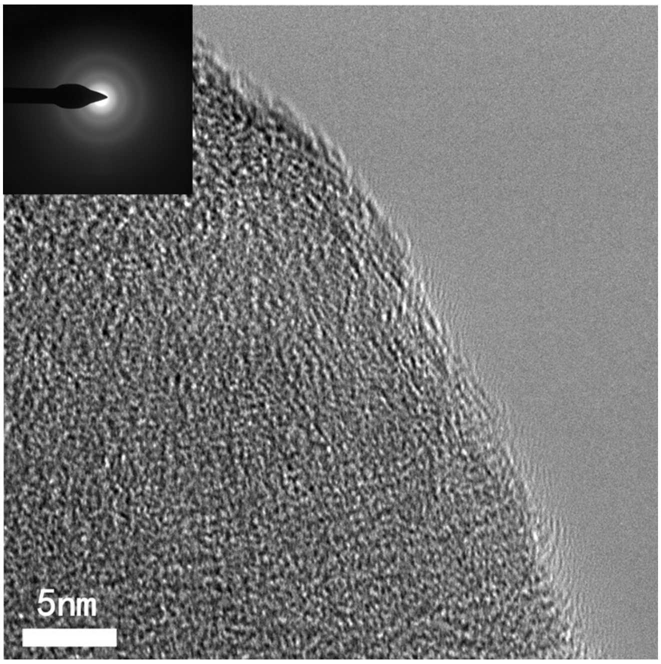

Figure S2. HRTEM image of HMCS (the inset is SAED patterns).

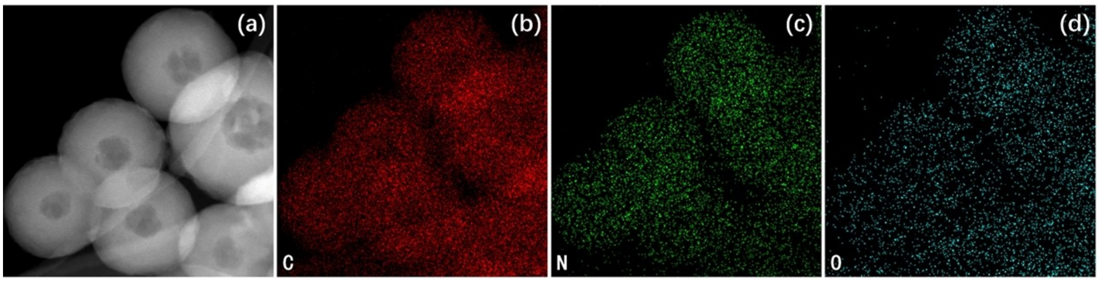

Figure S3. (a-d) HAADF analysis and mapping of HMCS.

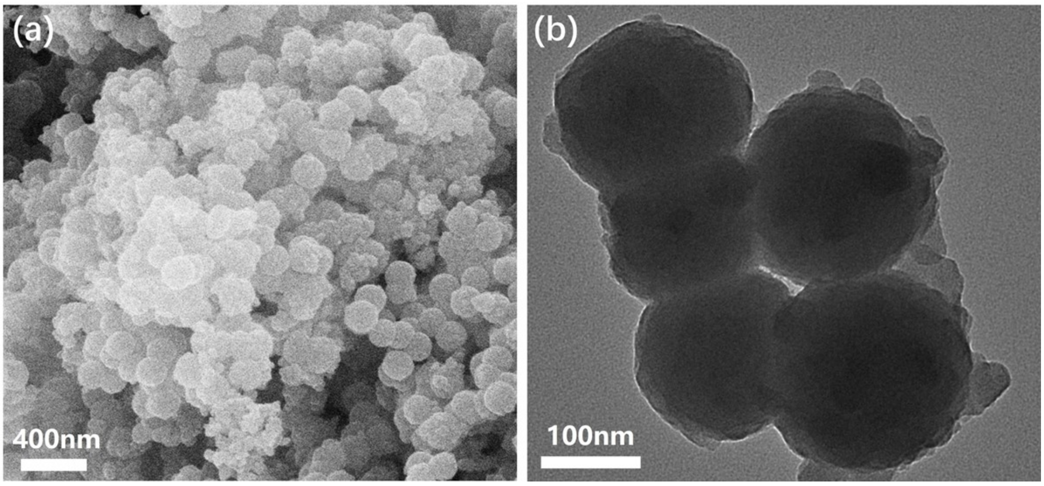

Figure S4. (a) SEM image of Ex-Sn@HMCS, (b) TEM image of Ex-Sn@HMCS.

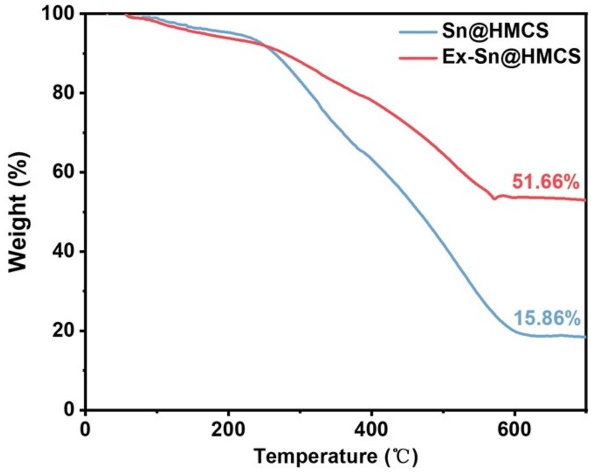

Figure S5. TG curves for Sn content measurement in Air.

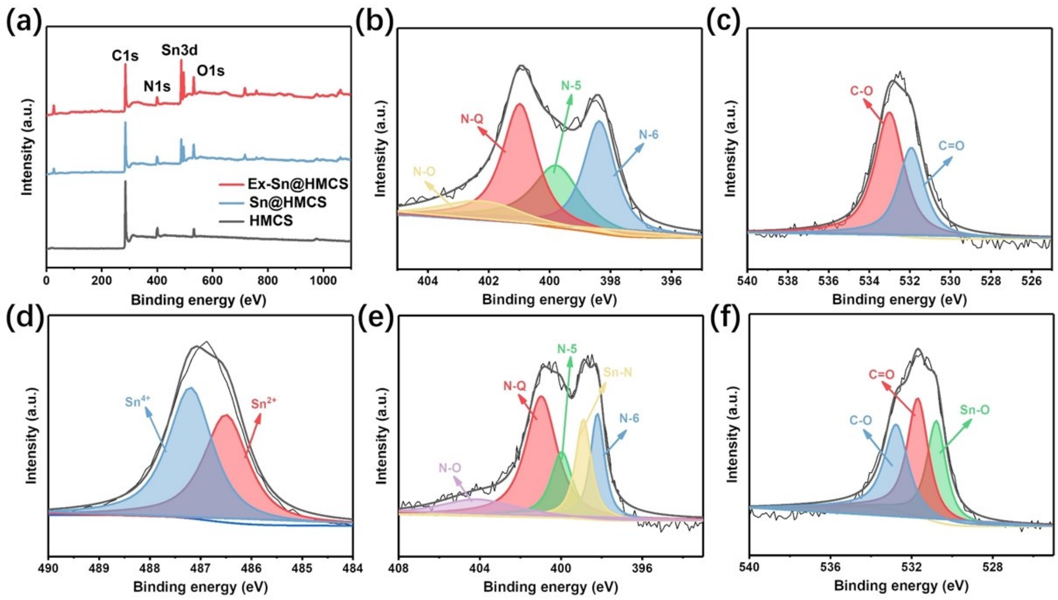

Figure S6. (a) XPS survey spectrum, (b) High-resolution XPS N1s spectra of HMCS, (c) High-resolution XPS O1s spectra of HMCS, (d) High-resolution XPS Sn 3d spectra of Sn@HMCS, (e) High-resolution XPS N1s spectra of Sn@HMCS, and (f) High-resolution XPS O1s spectra of Sn@HMCS.

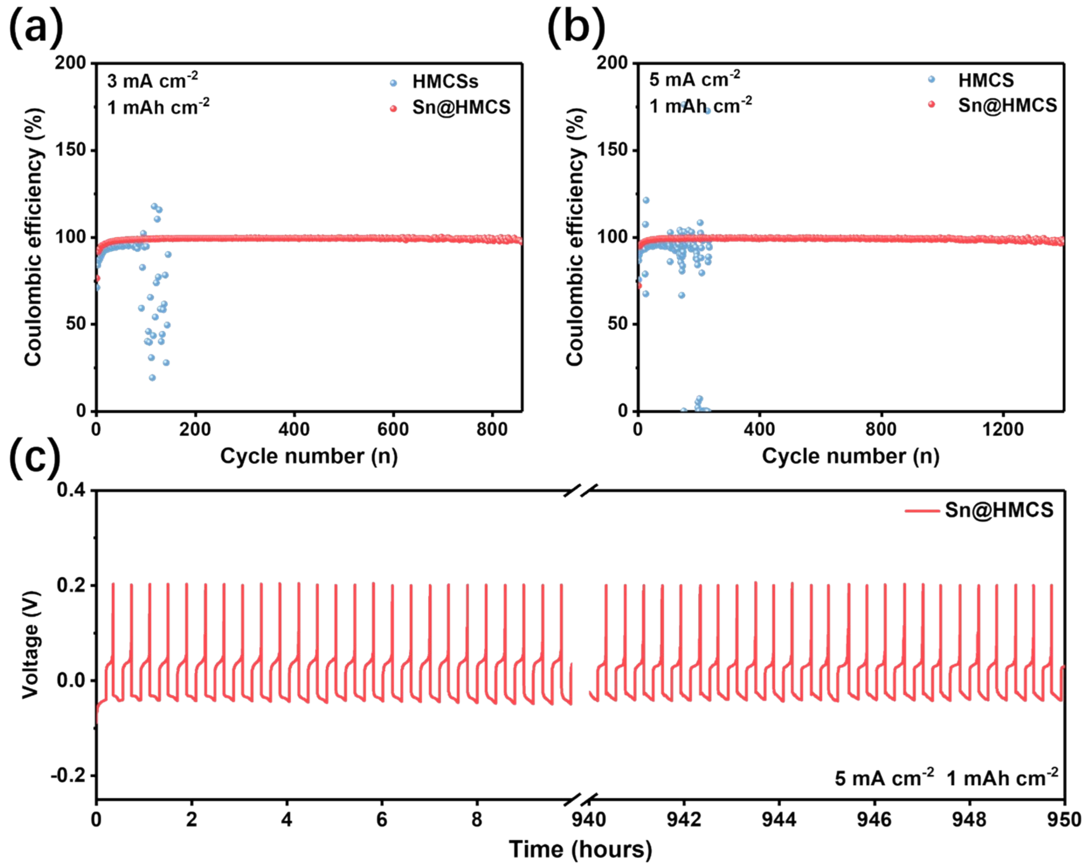

Figure S7. (a) Coulombic efficiencies at 3 mA cm^{-2} for 1 mAh cm^{-2}, (b) Coulombic efficiencies at 5 mA cm^{-2} for 1 mAh cm^{-2}, and (c) The voltage time curve at 5 mA cm^{-2} for 1 mAh cm^{-2}.

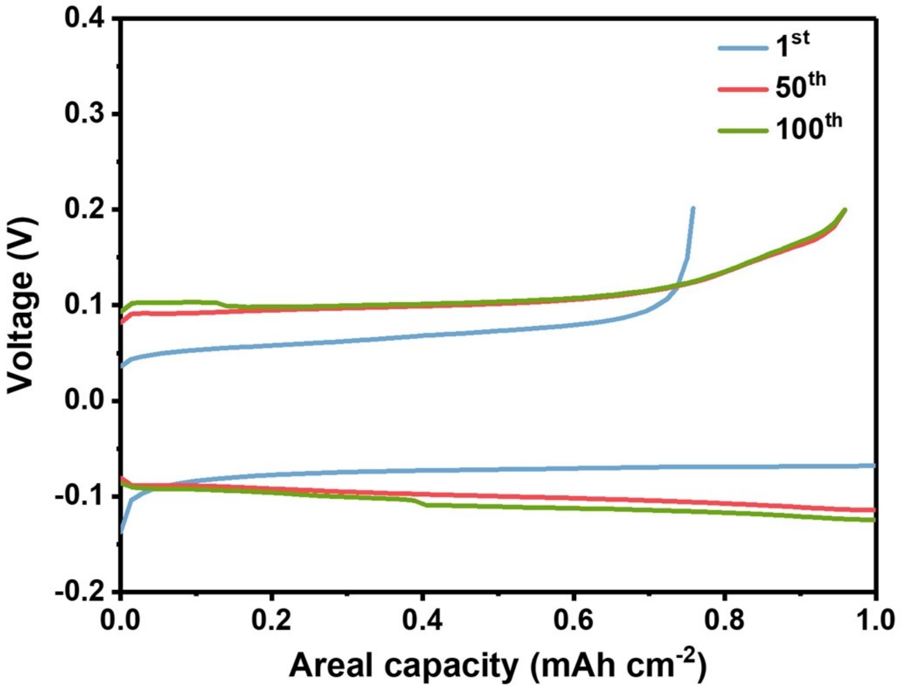

Figure S8. Voltage-Areal capacity curves of HMCS at 5 mA cm^{-2} for 1 mAh cm^{-2}.

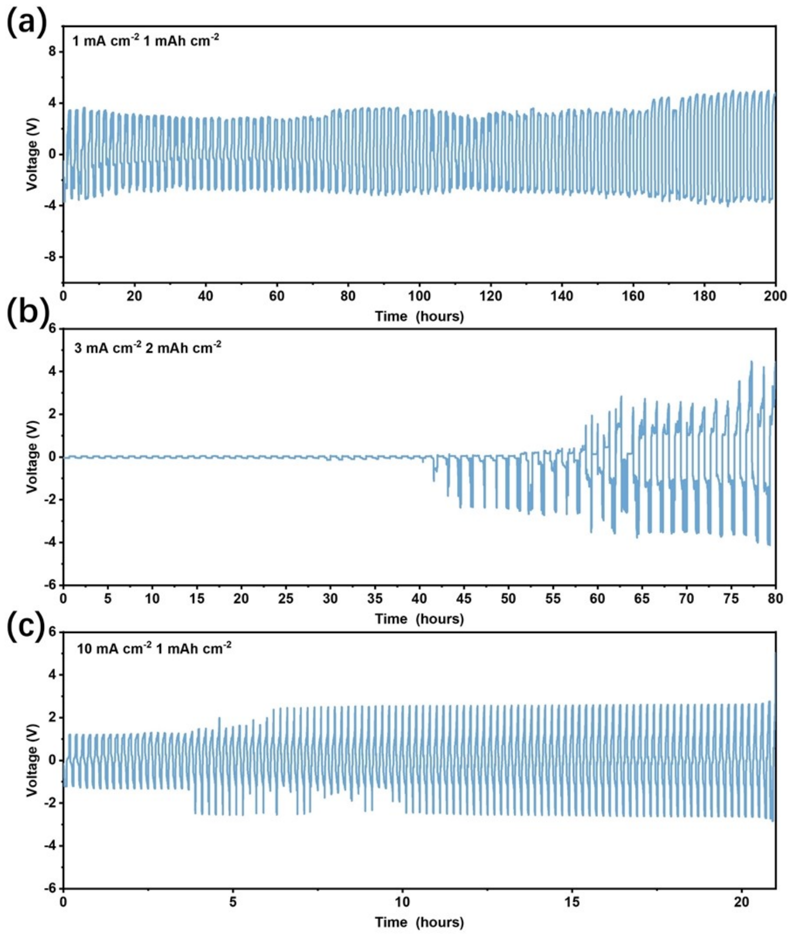

Figure S9. Voltage-time profiles of HMCS in symmetric cell at (a) 1 mA cm^{-2} for 1 mAh cm^{-2}, (b) 3 mA cm^{-2} for 2 mAh cm^{-2} and (c) 10 mA cm^{-2} for 1 mAh cm^{-2}.

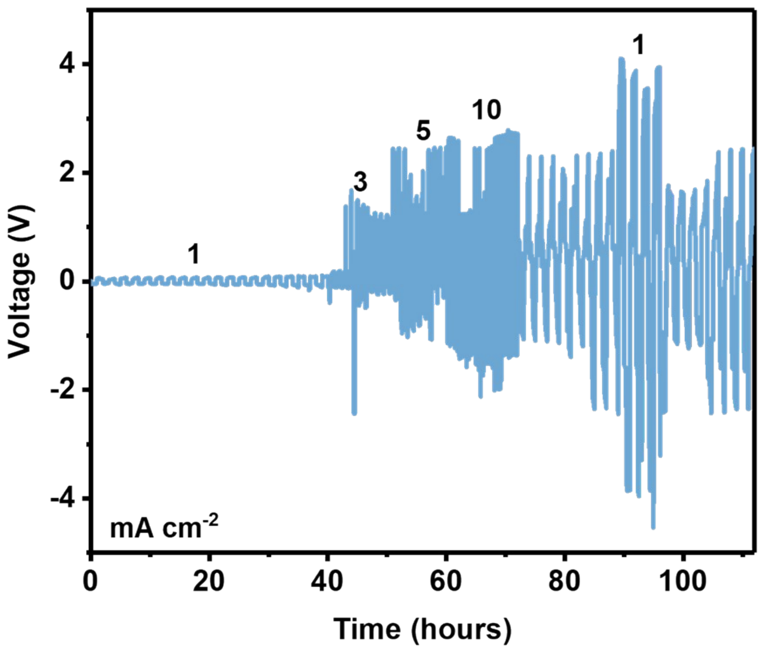

Figure S10. The rate performance of HMCS in symmetric cell.

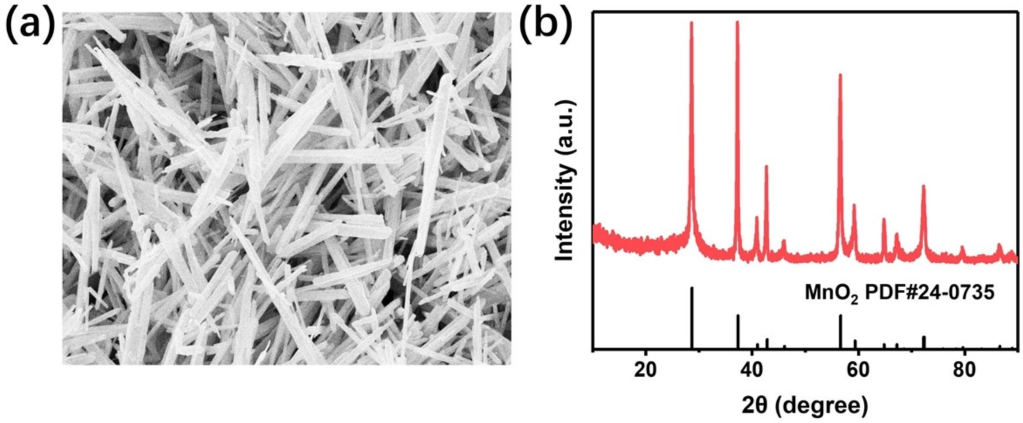

Figure S11. Characterization of synthetic manganese dioxide: (a) SEM image, (b) XRD pattern.

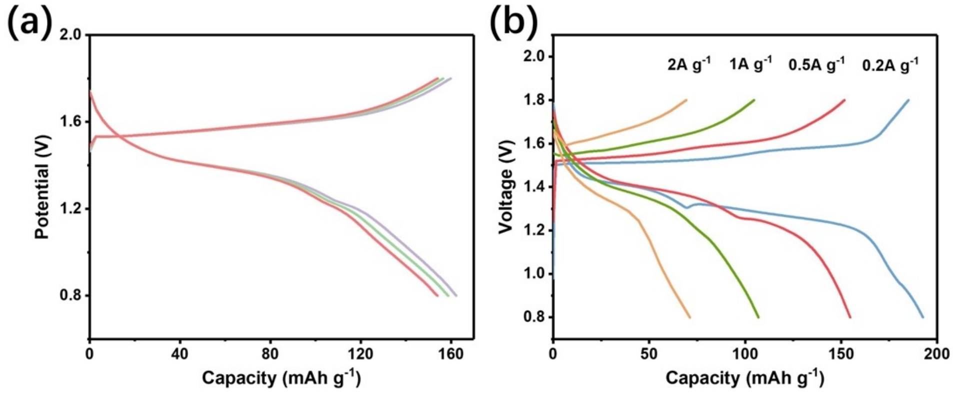

Figure S12. Electrochemical performance of Sn@HMCS in full cell: (a) GCD curves, (b) Capacity-voltage curves.

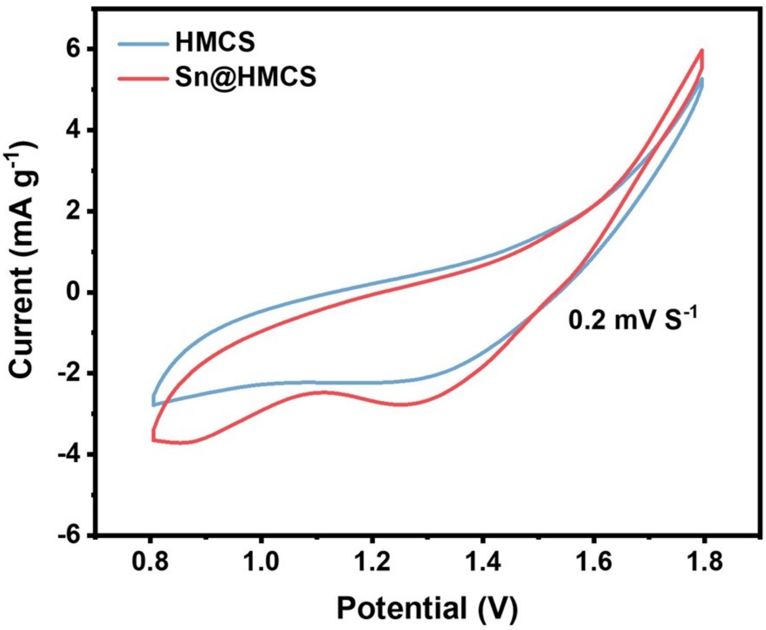

Figure S13. CV curves of Sn@HMCS and HMCS.

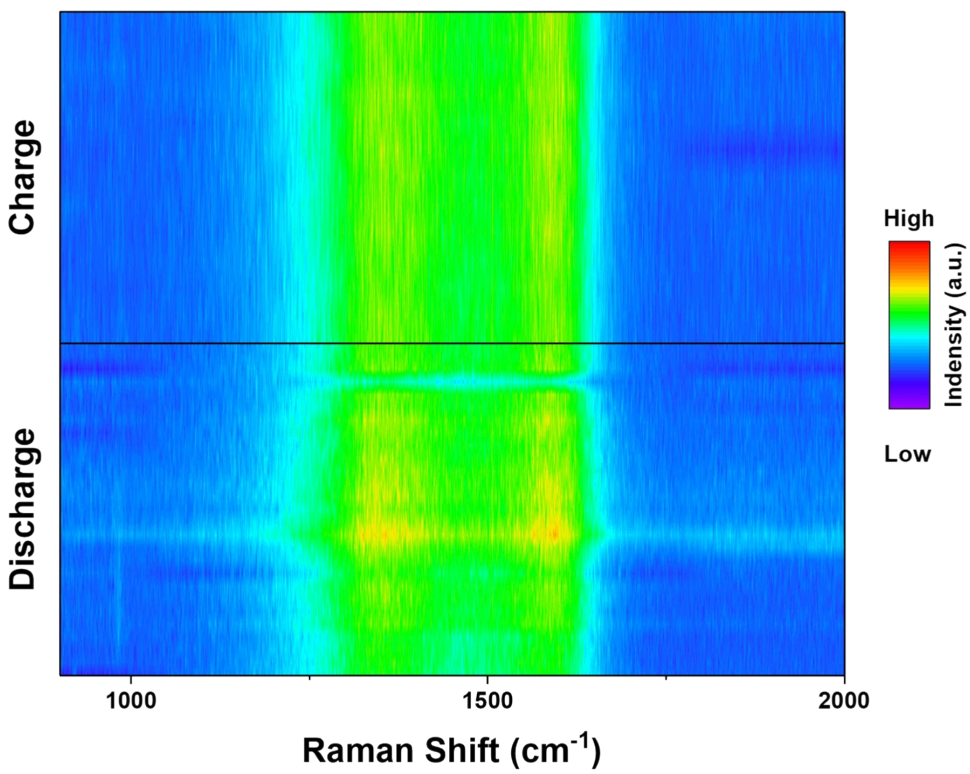

Figure S14. In situ Raman spectra of Sn@HMCS at 1A g^{-1} deposited for 2 hours.

Supporting Tables

Table S1. The contents of C, O, N and Sn in obtained samples (Average of two tests)

Sample	C at.%	O at.%	N at.%	Sn at.%
NMCSs	83.03	11.35	5.56	0
Sn-NMCSs	76.2	12.21	10.12	1.47

Table S2. Symmetrical cell performance comparison

	Current density (mA cm^{-2})	Area capacity (mAh cm^{-2})	Cycle life (h)
This Work	1	1	2400
	3	2	1120
	10	1	300
Flower-shaped carbon[2]	1	1	250
	10	1	500
Metal-organic frameworks-Zn[3]	1	1	1100
	5	5	400
	10	1	180
Zn@Carbon nanotube[4]	1	1	600
	2	1	1050
Anchored-$BaTiO_3$-separator[5]	0.5	0.25	2000
	2	1	1050
	5	2.5	150
Graphene carpet[6]	0.5	0.25	500
	2	1	500
Polarized ferroelectric	1.8	0.45	100
polymer material[7]	4.4	1.1	1200
$BaTiO_3$-coated Zn layer[8]	0.4	0.2	1600
	1	0.5	400

Table S3. Full cell performance comparison

Reference	Current density ($A\ g^{-1}$)	Cycle life (h)
This Work	1	900
Flower-shaped carbon[2]	5	250
$BaTiO_3$-coated Zn layer[8]	2	300
Cerium-based Conversion Film[9]	0.5	400
Uniform-Porous Kaolin Layer[10]	0.5	600
Tetramethylammonium Chloride layer[11]	0.02	200
Zn-modified H-form Zeolite[12]	1	800
Polypyrrole coating[13]	1	200

References

1. Liu, L.; Lu, Y.; Wang, S.; Ding, Y.; Chen, Y.; Qiu, D.; Wang, D.; Niu, J.; Zhang, J.; Chen, X.; Song, H., B, N Stabilization Effect on Multicavity Carbon Microspheres for Boosting Durable and Fast Potassium-Ion Storage. *Journal of Colloid and Interface Science* **2022,** *620* (15), 24-34.
2. Xu, Z.; Jin, S.; Zhang, N.; Deng, W.; Seo, M. H.; Wang, X., Efficient Zn Metal Anode Enabled by O,N-Codoped Carbon Microflowers. *Nano Lett* **2022,** *22* (3), 1350-1357.
3. Zhao, C.; Du, Y.; Guo, Z.; Chen, A.; Liu, N.; Lu, X.; Fan, L.; Zhang, Y.; Zhang, N., Missing-linker bifunctional MIL-125(Ti)-Zn interface modulation layer to simultaneously suppress hydrogen evolution reaction and dendrites for Zn metal anodes. *Energy Storage Materials* **2022,** *53*, 322-330.
4. Dong, L.; Yang, W.; Yang, W.; Tian, H.; Huang, Y.; Wang, X.; Xu, C.; Wang, C.; Kang, F.; Wang, G., Flexible and conductive scaffold-stabilized zinc metal anodes for ultralong-life zinc-ion batteries and zinc-ion hybrid capacitors. *Chemical Engineering Journal* **2020,** *384*.
5. Liang, Y.; Ma, D.; Zhao, N.; Wang, Y.; Yang, M.; Ruan, J.; Yang, G.; Mi, H.; He, C.; Zhang, P., Novel Concept of Separator Design: Efficient Ions Transport Modulator Enabled by Dual-Interface Engineering Toward Ultra-Stable Zn Metal Anodes. *Advanced Functional Materials* **2022,** *32* (25).
6. Li, C.; Sun, Z.; Yang, T.; Yu, L.; Wei, N.; Tian, Z.; Cai, J.; Lv, J.; Shao, Y.; Rummeli, M. H.; Sun, J.; Liu, Z., Directly Grown Vertical Graphene Carpets as Janus Separators toward Stabilized Zn Metal Anodes. *Adv Mater* **2020,** *32* (33), e2003425.

7. Wang, Y.; Guo, T.; Yin, J.; Tian, Z.; Ma, Y.; Liu, Z.; Zhu, Y.; Alshareef, H. N., Controlled Deposition of Zinc-Metal Anodes via Selectively Polarized Ferroelectric Polymers. *Adv Mater* **2022,** *34* (4), e2106937.
8. Wu, K.; Yi, J.; Liu, X.; Sun, Y.; Cui, J.; Xie, Y.; Liu, Y.; Xia, Y.; Zhang, J., Regulating Zn Deposition via an Artificial Solid-Electrolyte Interface with Aligned Dipoles for Long Life Zn Anode. *Nanomicro Lett* **2021,** *13* (1), 79.
9. Deng, C.; Xie, X.; Han, J.; Lu, B.; Liang, S.; Zhou, J., Stabilization of Zn Metal Anode through Surface Reconstruction of a Cerium-Based Conversion Film. *Advanced Functional Materials* **2021,** *31* (51).
10. Deng, C.; Xie, X.; Han, J.; Tang, Y.; Gao, J.; Liu, C.; Shi, X.; Zhou, J.; Liang, S., A Sieve-Functional and Uniform-Porous Kaolin Layer toward Stable Zinc Metal Anode. *Advanced Functional Materials* **2020,** *30* (21).
11. Xu, Y.; Zheng, X.; Sun, J.; Wang, W.; Wang, M.; Yuan, Y.; Chuai, M.; Chen, N.; Hu, H.; Chen, W., Nucleophilic Interfacial Layer Enables Stable Zn Anodes for Aqueous Zn Batteries. *Nano Lett* **2022,** *22* (8), 3298-3306.
12. Lin, X.-S.; Sun, J.-R.; Ge, L.-H.; Xu, J.-W.; Liu, W.-L.; Ren, M.-M.; Kong, F.-G.; Wang, S.-J.; Zhang, C.-B., Zn-modified zeolites host for dendrite-free zinc metal anodes. *Journal of Sol-Gel Science and Technology* **2022,** *103* (2), 386-395.
13. Zhang, F.; Wang, C.; Pan, J.; Tian, F.; Zeng, S.; Yang, J.; Qian, Y., Polypyrrole-controlled plating/stripping for advanced zinc metal anodes. *Materials Today Energy* **2020,** *17*.